

Casimir interactions in graphene systems

Bo E Sernelius

Linköping University Post Print

N.B.: When citing this work, cite the original article.

Original Publication:

Bo E Sernelius , Casimir interactions in graphene systems, 2011, Europhysics letters, (95), 5, 57003.

<http://dx.doi.org/10.1209/0295-5075/95/57003>

Copyright: Institute of Physics / EDP Sciences

<http://publications.edpsciences.org/>

Postprint available at: Linköping University Electronic Press

<http://urn.kb.se/resolve?urn=urn:nbn:se:liu:diva-70547>

Casimir interactions in graphene systems

Bo E. SERNELIUS

Division of Theory and Modeling, Department of Physics, Chemistry and Biology, Linköping University - SE-581 83 Linköping, Sweden

PACS 73.21.-b – Electron states and collective excitations in multilayers, quantum wells, mesoscopic, and nanoscale systems

PACS 71.10.-w – Theories and models of manyelectron systems

PACS 73.22.Pr – Electronic structure of graphene

Abstract. - The non-retarded Casimir interaction (van der Waals interaction) between two free standing graphene sheets as well as between a graphene sheet and a substrate is determined. We present several different derivations of the interaction. An exact analytical expression is given for the dielectric function of graphene along the imaginary frequency axis within the random phase approximation for arbitrary frequency, wave vector, and doping.

The first reference to the material graphene in the literature was made by Boehm et al. [1] in 1962. With modern technology it is now possible to produce large area graphene sheets and graphene has become one of the most advanced two-dimensional (2D) materials of today. Due to its superior transport properties it has a high potential for technological applications [2–6]. A free standing graphene sheet has a very interesting band structure. The valence and conduction bands form two sets of cones. In each set the two cones are aligned above each other with their tips coinciding at the fermi level. Thus, the fermi surface is just two points in the Brillouin zone; the value of the band gap is zero. The energy dispersion in the conduction and valence bands is linear which means that the carriers behave as relativistic particles with zero rest mass. When a graphene layer is formed on a substrate the fermi level moves up or down in energy — the sheet is doped.

A graphene layer interacts with other graphene layers or with a substrate with Casimir forces, forces that were predicted [7] by Casimir in 1948. In a pioneering work Sparnaay [8] tried to experimentally verify the existence of the Casimir force between two parallel plates. However, the experimental uncertainties were of the same order of magnitude as the force itself so the experiment was non-conclusive. The interest in the Casimir force virtually exploded a decade ago. This increase in interest was triggered by a torsion pendulum experiment by Lamoreaux [9], which produced results with good enough accuracy for the comparison between theory and experiment

to be feasible. This stimulated both theorists [10–15] and experimentalists [16–19] and the Casimir field has grown constantly since then. The thermal Casimir effect is not completely understood yet [20,21]. These forces are very important in graphene systems. They are the result of many-body interactions. Other many-body effects modify the dispersion of the energy bands [22–27]. The present work is devoted to the forces.

We derive the Casimir interaction between two graphene sheets, undoped and doped, and between one graphene sheet and a substrate. Numerical results are presented in the range from 1\AA to $1\mu\text{m}$ for experimentally relevant doping concentrations. The derivations are performed within the non-retarded formalism. It was demonstrated in Ref. [28] that retardation effects are not important in undoped graphene. For doped graphene retardation effects are expected to show up at separations outside the range considered here. Furthermore, we present explicit expressions for the dielectric function of doped graphene on the imaginary frequency axis, in terms of real valued functions of real valued variables.

We begin by calculating the interaction energy between two graphene layers. For undoped graphene retardation effects never show up [28] because of the particular band structure. For doped graphene they do for large enough separation. We limit the calculation to small enough separations for the retardation effects to be negligible. **An estimate of the separation at which retardation effects become important is the separation where the non-**

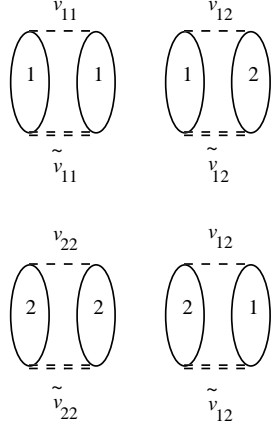


Fig. 1: Feynman diagrams for the correlation energy in the two graphene sheet system. The ellipses represent polarization bubbles and the dashed lines the interactions indicated in the figure. The numbers 1 and 2 refer to which sheet the electron belongs to. See [29] for details.

retarded result crosses the result for two perfectly reflecting metal half spaces, $E(d) = -\hbar c \pi^2 / (720 d^3)$. For undoped graphene this crossing never occurs. For doped graphene it occurs and earlier the higher the doping concentration. For the doping concentration $1 \times 10^{13} \text{ cm}^{-2}$, which is the highest considered in this work, the crossing occurs at approximately $300 \mu\text{m}$. We present results for separations smaller than $1 \mu\text{m}$ so we are well within the non-retarded regime. Thus we calculate the non-retarded Casimir interaction or in other words the van der Waals interaction. The interaction energy is then nothing but the inter-layer correlation energy [29]. At zero temperature it is given by

$$E_c(d) = \frac{\hbar}{(2\pi)^2} \int_0^\infty \int_0^\infty d\omega dq q \ln \left\{ 1 - e^{-2qd} \left[\frac{\alpha'(q, \omega)}{1 + \alpha'(q, \omega)} \right]^2 \right\}, \quad (1)$$

where $\alpha(q, \omega)$ is the polarizability of one graphene layer. The prime indicates that the function is calculated along the imaginary axis of the complex frequency plane. In terms of the polarizability the dielectric function is given by $\varepsilon(q, \omega) = 1 + \alpha(q, \omega) = 1 - v^{2D}(q) \chi(q, \omega) / \kappa$, where $v^{2D}(q) = 2\pi e^2 / q$ is the 2D fourier transform of the coulomb potential, κ is the dielectric constant of the surrounding medium, and $\chi(q, \omega)$ the density-density correlation function or polarization bubble. The feynman diagrams representing this energy are given in Fig. 1. The force is obtained as minus the derivative of the energy with respect to separation, d , i.e.,

$$F_c(d) = \frac{\hbar}{2\pi^2} \int_0^\infty \int_0^\infty d\omega dq q^2 \left\{ 1 - e^{+2qd} \left[\frac{1 + \alpha'_0(q, \omega)}{\alpha'_0(q, \omega)} \right]^2 \right\}^{-1}. \quad (2)$$

Let us first begin with an undoped graphene sheet. In a general point in the complex frequency plane, away from

the real axis the density-density correlation function is [30]

$$\chi(\mathbf{q}, z) = -\frac{g}{16\hbar} \frac{q^2}{\sqrt{v^2 q^2 - z^2}}, \quad (3)$$

where v is the carrier velocity which is a constant in graphene ($E = \pm \hbar v k$), and g represents the degeneracy parameter with the value of 4 (a factor of 2 for spin and a factor of 2 for the cone degeneracy.) With this particular screening it turns out that $\alpha'(\mathbf{q}/\lambda, \omega/\lambda) = \alpha'(\mathbf{q}, \omega)$ and the separation dependence of the interaction becomes very simple. A change of dummy variables results in

$$E_c(d) = \frac{1}{d^3} \frac{\hbar}{(2\pi)^2} \int_0^\infty \int_0^\infty d\omega dq q \ln \left\{ 1 - e^{-2q} \left[\frac{\alpha'(q, \omega)}{1 + \alpha'(q, \omega)} \right]^2 \right\} \\ \approx 2.156 \frac{1}{d^3} J / m^2, \quad (4)$$

with the value for v chosen [31] to be $8.73723 \times 10^5 \text{ m/s}$; d is the distance in \AA .

When the graphene sheet is doped the expression for the density-density correlation function is much more complicated. The retarded version has independently been obtained by Hwang and Das Sarma [32] and by Wunsch [31] et al. Here we present our general expression in the complex frequency plane, away from the real axis. In particular we give the result on the imaginary axis, which is where we perform the present calculations. We, just as in [31, 32], include the contribution from the conduction and valence bands, only, and assume that the linear dispersion, ($E = \pm \hbar v k$), of the bands extends forever. In the real system the dispersion starts to deviate from linear at some point and transitions from the occupied core states to empty bands higher up in energy will contribute to some extent to the screening. We neglect this here. The linear dispersion should be a good approximation for $|E| \leq 3 \text{ eV}$. Deviations from the linear dispersion are generally expected to modify the results at the low separation limit of the range we cover here.

In the two next equations we use dimension-less variables: $x = q/2k_F$; $y = \hbar\omega/4E_F$; $\tilde{z} = \hbar z/4E_F$. The density-density correlation function in a general point in the complex frequency plane, away from the real axis is

$$\chi(\mathbf{q}, z) = -D_0 \left\{ 1 + \frac{x^2}{4\sqrt{x^2 - \tilde{z}^2}} [\pi - f(x, \tilde{z})] \right\}; \\ f(x, \tilde{z}) = \text{asin} \left(\frac{1 - \tilde{z}}{x} \right) + \text{asin} \left(\frac{1 + \tilde{z}}{x} \right) \\ - \frac{\tilde{z} - 1}{x} \sqrt{1 - \left(\frac{\tilde{z} - 1}{x} \right)^2} + \frac{\tilde{z} + 1}{x} \sqrt{1 - \left(\frac{\tilde{z} + 1}{x} \right)^2}. \quad (5)$$

The same result holds for excess of electrons and excess of holes. The expression in Eq. (5) reproduces the results of Refs. [31, 32] when z approaches the real axis from above, apart from an anomaly in the result of Ref. [32]. The expression in their Eq. (8), which should be purely real has an imaginary part. If this is removed their result agrees with both ours and that in Ref. [31].

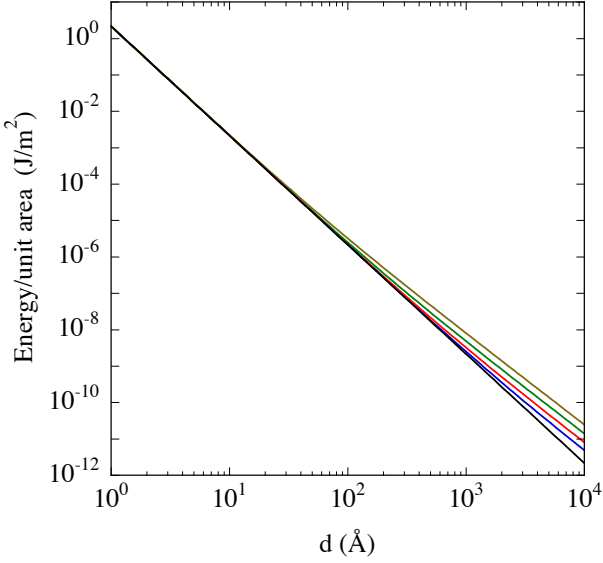


Fig. 2: The attractive interaction energy between two graphene sheets. The straight line is for undoped sheets, while the bent curves are for doping densities 1×10^{10} , 1×10^{11} , 1×10^{12} , and $1 \times 10^{13} \text{ cm}^{-2}$, respectively, counted from below.

The result on the imaginary axis can be expressed as

$$\begin{aligned} \chi'(\mathbf{q}, \omega) &= \chi(\mathbf{q}, i\omega) \\ &= -D_0 \left\{ 1 + \frac{x^2}{4\sqrt{y^2+x^2}} [\pi - g(x, y)] \right\}; \\ g(x, y) &= \text{atan} [h(x, y)k(x, y)] + l(x, y); \\ h(x, y) &= \frac{2 \left\{ [x^2(y^2-1) + (y^2+1)^2] + (2yx^2)^2 \right\}^{1/4}}{\sqrt{(x^2+y^2-1)^2 + (2y)^2 - (y^2+1)}}, \\ k(x, y) &= \sin \left\{ \frac{1}{2} \text{atan} \left[\frac{2yx^2}{x^2(y^2-1) + (y^2+1)^2} \right] \right\}, \\ l(x, y) &= \frac{\sqrt{-2x^2(y^2-1) - 2(y^4 - 6y^2 + 1) + 2(y^2+1)\sqrt{x^4 + 2x^2(y^2-1) + (y^2+1)^2}}}{x^2}, \end{aligned} \quad (6)$$

where the arcus tangens function is taken from the branch where $0 \leq \text{atan} < \pi$, $D_0 = \sqrt{gn/\pi v^2}$ is the density of states at the fermi level and n is the doping concentration. The density-density correlation function on the imaginary frequency axis has been derived before in a compact **and inexplicit** form (see Ref. [33] and references therein.) Here we have chosen to express it **in an explicit form** in terms of real valued functions of real valued variables.

The numerical results for the size of the interaction energy between two undoped graphene layers in vacuum is shown as the straight line in Fig. 2. The bent curves are valid for doping concentrations 1×10^{10} , 1×10^{11} , 1×10^{12} , and $1 \times 10^{13} \text{ cm}^{-2}$, respectively, counted from below. The interaction energy is negative, leading to an attractive force.

The interaction between two 2D metallic sheets was derived in [29]. To illustrate the difference between the two systems we show in Fig. 3 the corresponding results for two 2D metallic sheets in vacuum for the same set of carrier

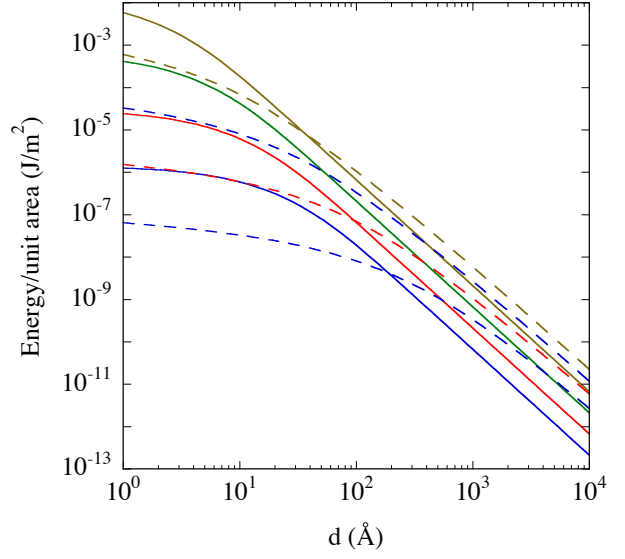


Fig. 3: The attractive interaction energy between two 2D metallic layers (solid curves). The broken curves show the contribution to the energy from the doping carriers in Fig. 2. Both sets of curve are for doping densities 1×10^{10} , 1×10^{11} , 1×10^{12} , and $1 \times 10^{13} \text{ cm}^{-2}$, respectively, counted from below.

concentrations; we have used the effective mass unity for the carriers.

According to Langbein [34] the correct asymptotic power law for the interaction between two objects should be obtained by simply using summation over pair interactions, but the actual strength of the interaction could not be obtained this way. For two parallel thin films this gives the power law d^{-4} (d^{-5}) in the non-retarded (retarded) limit. We found in [29] that this is not true for a pair of 2D metallic sheets. We found a fractional power law, $d^{-5/2}$, in the non-retarded limit (see the straight part of the solid curves in Fig. 3) and the power law d^{-3} in the retarded. Here, we have a system with yet another separation dependence. For a pair of undoped graphene layers the non-retarded interaction varies as d^{-3} , verifying the prediction by Dobson et al. [35], and the same power law holds in the retarded regime. This is the same power law as for the retarded interaction between two half spaces. The origin of the half-integer behavior for the 2D metal sheets is the square root dependence of the dispersion curve for 2D plasmons. In doped graphene the plasmon dispersion curve attains the square root dependence and for larger separations the interaction varies as $d^{-5/2}$ (see the right-most part of Figs. 2 and 3). For small enough separations the contribution to the interaction from the free carriers shows a much weaker separation dependence. This is obvious in both Figs. 2 and 3. The change in character occurs at a separation of the order of the Thomas Fermi screening length.

Before we treat next geometry which is a graphene sheet above a substrate it is illustrative to rederive Eq. (1) in

a different way. In [29] we derived it in two alternative ways; here we do it in yet another way. Let us assume that we have an induced carrier distribution, $\rho_1(\mathbf{q}, \omega)$, in sheet 1. This gives rise to the potential $v(\mathbf{q}, \omega) = v^{2D}(q) \rho_1(\mathbf{q}, \omega)/\kappa$ and $\exp(-qd) v^{2D}(q) \rho_1(\mathbf{q}, \omega)/\kappa$ in sheets 1 and 2, respectively. The resulting potential in sheet 2 after screening by the carriers is $\exp(-qd) v^{2D}(q) \rho_1(\mathbf{q}, \omega)/\{\kappa[1 + \alpha(\mathbf{q}, \omega)]\}$, which gives rise to an induced carrier distribution in sheet 2,

$$\rho_2(\mathbf{q}, \omega) = \chi(\mathbf{q}, \omega) e^{-qd} v^{2D}(q) \frac{\rho_1(\mathbf{q}, \omega)}{\kappa [1 + \alpha(\mathbf{q}, \omega)]}. \quad (7)$$

In complete analogy, this carrier distribution in sheet 2 gives rise to a carrier distribution in sheet 1,

$$\rho_1(\mathbf{q}, \omega) = \chi(\mathbf{q}, \omega) e^{-qd} v^{2D}(q) \frac{\rho_2(\mathbf{q}, \omega)}{\kappa [1 + \alpha(\mathbf{q}, \omega)]}. \quad (8)$$

To find the condition for self-sustained fields, normal modes, we let this induced carrier density in sheet 1 be the carrier density we started from. This leads to

$$1 - e^{-2qd} \left[\frac{\alpha(\mathbf{q}, \omega)}{1 + \alpha(\mathbf{q}, \omega)} \right]^2 = 0. \quad (9)$$

The left hand side of this equation is exactly the argument of the logarithm in Eq. (1). Eq. (1) was derived using many-body theory. In [36] the interaction energy is derived from the electromagnetic normal modes of the system. One ends up with an identical expression to the one in Eq. (1) where now the argument of the logarithm is the function in the condition for normal modes.

If we have a 2D layer (like a graphene sheet) the distance d above an ideal (perfectly reflecting) metal substrate the procedure is very similar. We start with an induced mirror carrier density, $\rho_1(\mathbf{q}, \omega)$, in the substrate. The induced carrier density in the graphene sheet is given by the expression in Eq. (7) except that now the distance between the mirror charge and the graphene layer is $2d$ instead of d . Eq. (8) is then replaced by $\rho_1(\mathbf{q}, \omega) = -\rho_2(\mathbf{q}, \omega)$, according to the result for a mirror charge at an ideal-metal interface. The condition for modes becomes

$$1 - e^{-2qd} \frac{\alpha(\mathbf{q}, \omega)}{1 + \alpha(\mathbf{q}, \omega)} = 0, \quad (10)$$

resulting in the energy

$$E_c(d) = \frac{\hbar}{(2\pi)^2} \int_0^\infty \int_0^\infty d\omega dq q \ln \left\{ 1 - e^{-2qd} \left[\frac{\alpha'(q, \omega)}{1 + \alpha'(q, \omega)} \right] \right\}. \quad (11)$$

Unfortunately, for a graphene layer above an ideal metal substrate the integral does not converge, without a frequency cutoff; the polarizability dies off too slowly with frequency; the integrand varies as $1/\omega$ for large frequencies. Thus the approximation that the linear dispersion of the graphene conduction and valence bands extends forever is not applicable in this model system. For a 2D

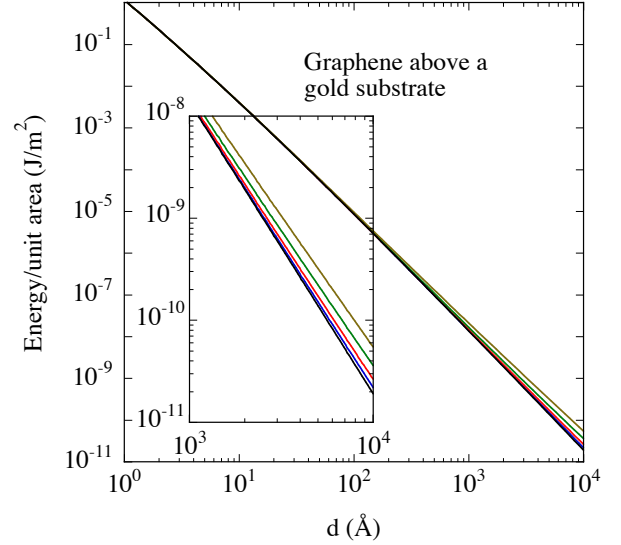


Fig. 4: The attractive interaction energy between a graphene sheet and a gold substrate. The lowest curve is for an undoped sheet, while the other curves are for doping densities 1×10^{10} , 1×10^{11} , 1×10^{12} , and $1 \times 10^{13} \text{ cm}^{-2}$, respectively, counted from below. The inset shows the expanded lower right part of the figure.

metallic sheet, on the other hand, above an ideal metal substrate there is no convergence problem.

Next we focus on a graphene layer above a real substrate. The derivation is the same as for an ideal metal substrate until the last step. Now, using the theory of image charges we realize that the relation between the induced carrier densities is

$$\rho_1(\mathbf{q}, \omega) = -\rho_2(\mathbf{q}, \omega) \frac{\varepsilon_s(\omega) - 1}{\varepsilon_s(\omega) + 1}, \quad (12)$$

and the condition for normal modes becomes

$$1 - e^{-2qd} \frac{\alpha(\mathbf{q}, \omega)}{1 + \alpha(\mathbf{q}, \omega)} \frac{\varepsilon_s(\omega) - 1}{\varepsilon_s(\omega) + 1} = 0. \quad (13)$$

Basically the same condition for modes was derived in a different way in Ref. [37]. We have neglected spatial dispersion in the substrate; inclusion of spatial dispersion would lead to a higher order of complexity [38, 39] and would have negligible effects on the present results. **To be noted is that spatial dispersion in the graphene sheet is fully taken into account.** From the condition in Eq. (13) follows that the interaction energy is given by

$$E_c(d) = \frac{\hbar}{(2\pi)^2} \int_0^\infty \int_0^\infty d\omega dq q \times \ln \left\{ 1 - e^{-2qd} \left[\frac{\alpha'(q, \omega)}{1 + \alpha'(q, \omega)} \frac{\varepsilon_{s'}(\omega) - 1}{\varepsilon_{s'}(\omega) + 1} \right] \right\}. \quad (14)$$

The result for a graphene sheet above a gold substrate is shown in Fig. 4. The dielectric function of gold along the imaginary frequency axis was obtained from experimental

data extrapolated in a way described in [10] and by the use of a modified Kramers Kronig dispersion relation (see Eq. (6.75) in [36].) The results presented in Figs. 2-4 become unreliable for separations smaller than the size of the graphene unit cell, i.e., for d values smaller than a couple of Å.

The lowest order term in various expansions of the interaction between a graphene layer and a totally reflecting metal half space has been derived in [40]. We stated earlier that the integral of Eq. (11) does not converge. It is a borderline case. It is very close to convergence. **To be more specific: For a given momentum the problem lies in the high frequency limit of the integrand. The integrand dies off as ω^{-1} , so the frequency integral is non-convergent. Had it instead died off as $\omega^{-(1+\delta)}$, where δ is an infinitesimal, the integral would have converged. By performing the integral in various prescribed ways or modifying the system the tiniest bit the integral can be made convergent.** In Ref. [40] the mass of a carrier in graphene was kept finite, not zero as in our treatment. This led to a well defined result for the interaction energy. Even the limit of the result as a function of mass when the mass goes to zero exists. In Ref. [41] the dielectric properties of graphene were treated in quite a different way. The conductivity was assumed to be $\sigma \equiv \sigma_0 = e^2/4\hbar$, and a fully retarded derivation yielded results very close to ours. The same power law for the interaction between two graphene sheets was found, and a similar value for the size of the interaction: 2.295 as compared to our value of 2.156 in Eq. (4). The binding energy of a graphene layer to different metal substrates obtained from density functional theory is reported in Ref. [42]. This energy has more contributions: kinetic energy gain from the redistribution of carriers between the sheet and the substrate; energy cost to build up the electrostatic fields due to the charging of the sheet; exchange and correlation energy changes due to the redistribution of the carriers. Thus comparison between our results is not feasible.

In summary, we have derived and calculated the Casimir interaction between two graphene sheets and between a graphene sheet and a substrate; for an ideal metal substrate the result is not finite if not a frequency cut off is introduced or some other regularization procedure is invoked. We found the interaction energy between two virgin graphene sheets varies with separation, d , as d^{-3} (the force as d^{-4} .) In contrast, summation over pair interactions for a pair of films leads to a d^{-4} dependence (the force as d^{-5} .) The interaction between doped graphene sheets has a more complex separation dependence. We see from the results that doping has a negligible effect on the force for small separations of the order of a nano meter but can lead to an order of magnitude increase at separations of the order of a micro meter. We have furthermore derived the dielectric function of graphene along the imaginary frequency axis within the random phase approximation for arbitrary frequency, wave vector, and doping. These results are needed for the present calcula-

tions and for future calculations of many-body effects in graphene.

REFERENCES

- [1] BOEHM H. P., CLAUSS, A., FISCHER G. O., and HOFMANN U., *Z. Naturforsch.* **17b** (1962)150.
- [2] NOVOSELOV K. S. , GEIM A. K., MOROZOV S. V., JIANG D., KATSNELSON M. I., GRIGORIEVA I. V., DUBONOS S. V., FIRSOV A. A., *Nature* **438** (2005) 197.
- [3] ZHANG Y., TAN Y.-W., STORMER H. L., KIM P., *Nature* **438** (2005) 201.
- [4] NOVOSELOV K. S., MCCANN E., MOROZOV S. V., FAL'KO V. I., KATSNELSON M. I., ZEITLER U., JIANG D., SCHEDIN F., and GEIM A. K., *Nature Phys.* **2** (2006) 177.
- [5] BERGER C., SONG Z., LI T., LI X., OGBAZGHI A. Y., FENG R., DAI Z., MARCHENKOV Z. N., CONRAD E. H., FIRST P. N., de HEER W. A., *J. Phys. Chem. B* **108** (2004) 19912.
- [6] VIROJANADARA C., SYVÄJARVI M., YAKIMOVA R., JOHANSSON L. I., ZAKHAROV A. A., and BALASUBRAMANIAN T., *Phys. Rev. B* **78** (2008) 245403.
- [7] CASIMIR H. B. G., *Proc. K. Ned. Akad. Wet.* **51** (1948) 793.
- [8] SPARNAAY M. J., *Physica* **24** (1958) 751.
- [9] LAMOREAUX S. K., *Phys. Rev. Lett.* **78**, 5 (1997).
- [10] BOSTRÖM M. and SERNELIUS Bo E., *Phys. Rev. Lett.* **84** (2000) 4757.
- [11] LAMBRECHT A., and REYNAUD S., *Eur. Phys. J. D* **8** (2000) 309.
- [12] BORDAG M., GEYER B., KLIMCHITSKAYA G. L., and MOSTEPANENKO V. M., *Phys. Rev. Lett.* **87** (2001) 259102.
- [13] BREVIK I., AARSETH J. B., and HØYE J. S., *Phys. Rev. E* **66** (2002) 026119.
- [14] SVETOVOY V. B., and LOKHANIN M. V., *Mod. Phys. Lett. A* **15** (2000) 1437.
- [15] NOGUEZ C., ROMÁN-VELÁZQUEZ C. E., ESQUIVEL-SIRVENT R., and VILLARREAL C., *Europhys. Lett.* **67** (2004) 191.
- [16] MOHIDEEN U., and ROY A., *Phys. Rev. Lett.* **81** (1998) 4549.
- [17] EDERTH T., *Phys. Rev. A* **62** (2000) 062104.
- [18] DECCA R. S., LÓPEZ D., FISCHBACH E., and KRAUSE D. E., *Phys. Rev. Lett.* **91** (2003) 050402.
- [19] BRESSI G., CARUGNO G., ONOFRIO R., and RUOSO G., *Phys. Rev. Lett.* **88** (2002) 041804.
- [20] SUSHKOV A. O., KIM W. J., DALVIT D. A. R., and LAMOREAUX S. K., *Nature Physics* **7** (2011) 230.
- [21] MILTON Kimball, *Nature Physics* **7** (2011) 190.
- [22] BOSTWICK A., OHTA T., SEYLLER T., HORN K., and ROTHENBERG E., *Nature Physics* **3** (2007) 36.
- [23] BERGGREN K.-F., and SERNELIUS Bo E., *Phys. Rev. B* **24** (1981) 1971.
- [24] SERNELIUS Bo E., *Phys. Rev. B* **34** (1986) 5610.
- [25] SERNELIUS Bo E., *Phys. Rev. B* **33** (1986) 8582.
- [26] SERNELIUS Bo E., *Phys. Rev. B* **36** (1987) 4878.
- [27] SHUNG Kenneth W. -K., SERNELIUS Bo E., MAHAN G. D., *Phys. Rev. B* **36** (1987) 4499.
- [28] GÓMEZ-SANTOS G., *Phys. Rev. B* **80** (2009) 245424.

- [29] SERNELIUS Bo E., and BJÖRK P., *Phys. Rev. B* **57** (1998) 6592.
- [30] GONZÁLES J., GUINEA F., and VOZMEDIANO M. A. H., *Nucl. Phys.* **424** (1994) 595.
- [31] WUNSCH B., STAUBER T., SOLS F., and GUINEA F., *New Journal of Physics* **8** (2006) 318.
- [32] HWANG E. H., and DAS SARMA S., *Phys. Rev. B* **75** (2007) 205418.
- [33] BARLAS Y., PEREG-BARNEA T., POLINI M., ASGARI R., and MACDONALD A. H., *Phys. Rev. Lett.* **98** (2007) 236601.
- [34] LANGBEIN D., *Theory of Van der Waals attraction*, (Springer, New York, 1974,) in the series Springer Tracts in Modern Physics.
- [35] DOBSON J. F., WHITE A., and RUBIO A., *Phys. Rev. Lett.* **96** (2006) 073201.
- [36] SERNELIUS Bo E., *Surface Modes in Physics* (Wiley-VCH, Berlin, 2001).
- [37] HORING Norman J. Morgenstern, *Phys. Rev. B* **80** (2009) 193401.
- [38] SERNELIUS Bo E., *Phys. Rev. B* **71** (2005) 235114.
- [39] SVETOVOY V. B., and ESQUIVEL R., *Phys. Rev. E* **72** (2005) 036113-1.
- [40] BORDAG M., FIALKOVSKY I. V., GITMAN D. M., and VASSILEVICH D. V., *Phys. Rev. B* **80** (2009) 245406.
- [41] DROSDOFF D., and WOODS Lilia M., *Phys. Rev. B* **82** (2010) 155459.
- [42] VANIN M., MORTENSEN J. J., KELKKANEN A. K., GARCIA-LASTRA J. M., THYGESEN K. S., and JACOBSEN K. W., *Phys. Rev. B* **81**(2010) 081408.